

The Third Spectrum of Tantalum (Ta III): Fine and Hyperfine Structure

V. I. Azarov^{*1}, W.-Ü L. Tchang-Brillet², J.-F. Wyart³ and F. G. Meijer⁴

¹Department of Research and Development, Parametric Technology Corporation, 140 Kendrick Street, Needham, MA 02494, USA

²Laboratoire d'Etude du Rayonnement et de la Matière en Astrophysique (LERMA), Observatoire de Paris-Meudon, 92190 Meudon, France, also Université Pierre et Marie Curie (Paris VI)

³Laboratoire Aime Cotton, CNRS (UPR3321), Bat 505, Centre Universitaire, 91405-Orsay, France

⁴Instituut voor Plasmafysica Rijnhuizen, Association Euratom-FOM, P.B. 1207, 3430 BE, Nieuwegein, The Netherlands, and SCFAB, KTH-Atomic and Molecular Physics, S-106 91 Stockholm, Sweden

Received August 26, 2002; accepted in revised form October 22, 2002

PACS ref: 31.15.Ct, 31.25.EB, 31.25.Jf, 31.30.Gs, 32.10.Fn, 32.30.Jc

Abstract

Presented is the first successful analysis of the Ta III spectrum. All the 37 levels of the low lying even configurations $5d^3$, $5d^26s$, and $5d6s^2$, and all the 68 levels of the higher odd configurations $5d^26p$ and $5d6s6p$ have been established. About 720 spectral lines have been classified in the region of 1000–3950 Å as belonging to the $(5d^3 + 5d^26s + 5d6s^2) - (5d^26p + 5d6s6p)$ transition array. The results are mainly based on spectrograms obtained by means of a vacuum sliding spark discharge and a 10.7 m normal incidence spectrograph at the Paris-Meudon Observatory, which provides a unique plate factor of 0.25 Å/mm in the first order. The resulting line list has been completed by partial data taken from earlier lists used for the Ta II and Ta IV studies. The analysis was guided by predicted energy level values and transition probabilities calculated by means of a complete set of orthogonal operators. The program suite IDEN for computer-aided spectra analyses played a crucial role in the study.

The list of classified spectral lines and derived energy level values are presented. Calculated energy values and Landé factors, LS -compositions and gA -values, obtained from the final fitted parameter values using the orthogonal operator approach are also given.

A few lines have partially resolved hyperfine structures owing to the high dispersion of the Meudon spectrograph. They connect levels with an unpaired 6s electron. The iso-nuclear trends of the a_{6s} hfs parameter are straight from Ta I to Ta III.

1. Introduction

Thanks to observations by the Goddard High Resolution Spectrograph (GHRS) on board the Hubble Space Telescope (HST) lines belonging to the spectra of 5d-elements have been identified in the chemically peculiar stars κ Cancri and χ Lupi [1]. It concerns especially the lower stages of ionization. As reported in the results of the “ χ Lupi Pathfinder Project” [2], abundances of Pt, Au and Hg in the star are 4–5 orders of magnitude higher than solar abundances. This renewed the interest for other 5d elements including tantalum.

The Ta III spectrum was the last third spectrum of all the non-radioactive elements left to be still unraveled. While the second, fourth, fifth and sixth tantalum spectra have been successfully studied in 1961–1978 [3–6], and the $5d5f-5d^2$ array has been recently classified in Ta IV [7], all attempts to establish the structure of any configuration of Ta III failed. Some lines from the list used for the Ta IV analysis [4] were tentatively attributed to Ta III. Furthermore, the spark spectrum measured by C. C. Kiess in the Ta II study [3] contains many unidentified lines that could

belong to Ta III. Therefore, its analysis appeared as a stimulating challenge and deserved new experimental data and the support of improved theoretical tools.

2. Experimental

The spectrum of Ta has been recorded in the 1200–2450 Å wavelength region on the 10.7 m VUV normal incidence spectrograph at the Paris-Meudon Observatory. This instrument is equipped with a 3600 lines/mm holographic grating and provides a unique plate factor of 0.25 Å/mm in the first order [8]. The ionized tantalum spectrum in emission was obtained using a vacuum sliding spark source with an anode made of a 99.9% pure tantalum rod. A 10 μ F capacitor was charged with a high voltage power supply delivering a voltage of 8 kV. To vary the discharge conditions, a self-inductance coil was placed in series with the spark source. For each wavelength region, two exposures were recorded with two values of the inductance, 68 μ H and 25 μ H in order to create “low” and “high” excitation conditions enhancing respectively lower (Ta III and Ta IV) and higher (Ta V and Ta VI) ionization stage emission. The anode was wrapped by a small piece of pure copper foil. The copper lines were used as internal standards for reducing the spectrograms. The plates were measured on a semi-automatic comparator equipped with a photoelectric device and connected to a linear fringe-counter, giving the plate position to $\pm 1 \mu$ m. The measurements have initially been reduced by means of O, C, Al, Cu and Ta IV lines present in the spectrograms. However, as explained in the next section, the precision of wavelengths can be improved during the course of analysis by considering their overall consistency. The final relative accuracy of the wavelengths is 0.004 Å in the 1200–2445 Å region. Above 2445 Å and below 1200 Å the unidentified lines from Kiess [3] and one of us [9] were used respectively. The spectrograms from Ref. [9] were originally obtained for the Ta IV study [4] with the 6.65 m normal incidence vacuum spectrograph at the Zeeman laboratory, University of Amsterdam, The Netherlands, equipped with a 1200 lines/mm grating. The accuracy of the lines above 2445 Å is about 0.017 Å. All the identified spectral lines were weighted according to their accuracy before they were used in the calculation of the energy level system. The calculation procedure is able to detect systematic errors in

* e-mail: vazarov@ptc.com

wavelengths of spectral lines used. Our analysis showed that the lines from Ref. [9] have a systematic error of 0.013 \AA with an additional random component of 0.010 \AA .

3. Parametric calculations

Energy parameter values obtained in neighboring spectra were used to estimate starting parameter values for the Ta III calculations. Recently, a careful consideration of trends of energy parameter values along the Yb I isoelectronic sequence with the $5d^2$ ground-state configuration was given [10]. The study showed quite regular evolution of the experimental parameters (or scaling factors of their *ab initio* values) along the sequence. Similar behavior was expected in the Lu I isoelectronic sequence, which consists of the ions having the $5d^3$ ground-state configuration and includes doubly ionized tantalum, Ta III. Some ions in the sequence have already been studied, viz. W IV, Re V, Os VI and Ir VII [11–15], thus providing a good starting point for the current analysis. It should be noticed that when the ionization stage lowers, the trends of parameters (or scaling factors of their *ab initio* values) become more irregular [10,16,17]. For instance, the mentioned factors for electrostatic parameters fall down sharply when we approach the third and second spectra. Also, the spectra of the lower stages of ionization are much more complex due to overlapping configurations in the even as well as in the odd system [17,18]. This, in part, is the reason why the Ta III spectrum has a long history of unsuccessful attempts to study.

The *ab initio* values of parameters needed for the purposes of extrapolation and estimation of starting parameter values for Ta III were calculated using the program developed by Cowan [19]. Calculations of energy level values and their eigenvector compositions were carried out by means of the orthogonal operator technique [16,20,21]. In these calculations the even system contained the $5d^3$, $5d^26s$ and $5d6s^2$ configurations, and the odd system included the $5d^26p$, $5d6s6p$ and $6s^26p$ configurations.

4. Computer aided analysis

The key instrument used in the analysis was the program suite IDEN [22,23]. A breakthrough was achieved by utilizing its module for the automatic search for energy levels. Input data for the code are lists of spectral lines, calculated energy levels and transition probabilities. Also specified are error bars for all the measured and all the calculated quantities, such as line wavelengths, energy level values and transition probabilities. Error bars for wavelengths may be given for separate lines and/or for parts of the line list. Random, as well as systematic errors may be specified. Moreover, one can specify a variety of constraints. Among them are the following:

- (i) Correlation of wavelength measurements. The error bars of the measured wavelength of a spectral line may consist of a specified systematic fraction and a random fraction. Obviously, a value of the interval between two very close but isolated spectral lines has an error derived only from the random errors of the two lines. The systematic fraction of the resulting error of the

calculated interval is then equal to zero. On the contrary, for distant, not correlated lines we have to combine systematic errors of both lines to form the resulting systematic error of the interval. To take this into account in calculations, we also give a maximal interval of correlation for a specified systematic error. In our code a list of pairs “systematic error—maximal interval of correlation” may be specified for any and each part of the wavelength list. The systematic error of the distance between two lines is calculated as a function of the distance. The parameters of the function are determined by the relevant specified pairs “systematic error—maximal interval of correlation”.

- (ii) Correlation of calculated energy levels. This is very important for calculation of error bars of intervals between energy levels. The error bars of the interval between two calculated levels may differ significantly depending on whether the levels belong to the same or different terms, to the same or different configurations. For example, the interval between two levels of a term of a configuration may be predicted with very high accuracy, though the configuration itself may be predicted with quite large uncertainty. This is because splitting of levels in a term, splitting of terms in a configuration and the average energy of the configuration are described by different parameters known with different accuracy. We have developed a simple way for specifying the whole error matrix reflecting correlation of all pairs of levels of the system under consideration.

The IDEN code first constructs a database and fills it with spectral lines pertinent for each allowed transition in accordance with the calculated transition probability, observed intensity, wavelength and other characteristics of lines, energy values of two levels involved, and also error bars specified for all these values. Then it performs reduction of the database (line selection, recalculation of error bars, etc.) by applying all the constraints that are intrinsic for the model, as well as all those that are specified. To speed up the process, a specially designed algorithm is used to apply the constraints in an optimal sequence. The current state of the problem solution can be examined in several ways. For example, the user may pick up the most developed transitions or levels, such as (a) those that contain the minimal number of possible variants of identification, e.g., with the least number of spectral lines pertinent for a transition, or (b) those that have minimal resulting (calculated after selection) error bars. Also, one may require to examine transitions or levels which are most sensitive to any changes in data or constraints related to them. Notable changes in such places will most probably result in significant changes in the data sets of other transitions/levels. During such a revision one may decide to change constraints or edit the data sets, e.g., edit a list of selected spectral lines for a transition. For instance, one may leave only one spectral line for a given transition and see if the whole system will survive the selection, i.e. if it will have at least one spectral line for each allowed transition. Initially we limit the automatic search by a set of levels connected by relatively strong calculated

transitions, introduce the constraints, and then gradually strengthen them in the course of an iterative procedure including database reduction and semiempirical recalculation of levels. Subsequently, moderate intensity transitions are added to the database. At the final stage we use the interactive routine of the IDEN suite to pick up the weakest spectral lines, to check identified lines having abnormally high intensity, to verify multiply identified and blended lines and to re-specify the wavelength accuracy for all these lines.

All the identified spectral lines were weighted according to their accuracy before they were used in the calculation of the energy level system. The calculation procedure is able to detect systematic errors in wavelengths of spectral lines used. Indeed, in the process of the analysis we found that our initially calculated wavelengths have regions with systematic deviations of up to 0.020 Å. Those were regions poor of standard lines and/or regions close to the edges of the photographic plates. This leads us to revise the standards and either carefully remeasure them or discard them if blended or saturated. At the same time we added some secondary standards obtained from the analysis: for some identified isolated lines we used calculated wavelengths derived from the very well determined energy levels. After finishing level searching we extended our list of classified lines above 2445 Å and below 1200 Å. The unidentified lines from Kiess [3] and Ref. [9] were used for this purpose, respectively. Comparison of line intensities from Kiess [3] and on our spectrograms in the overlapping wavelength region provided a criterion for selecting unidentified lines from Ref. [3] for Ta III. Indeed, these lines are rather weaker than the identified Ta II lines whereas they are stronger on our plates.

5. Results and discussion

As a result of the analysis, in the region of 1009–3944 Å, 724 spectral lines have been classified as belonging to the $(5d^3 + 5d^26s + 5d6s^2) - (5d^26p + 5d6s6p)$ transition array of Ta III. Nine lines are doubly classified. All identified lines and their classifications are given in Table I. In the first column of this table we give the theoretical transition probability, gA , for each identified transition. The second column shows the intensity of the spectral lines (Int) on a scale 1–250. The weakest spectral line detectable on Meudon's plates on the scale given is about 0.5. As can be seen, the agreement between gA and Int for the isolated unperturbed lines is quite good. The third, fourth, fifth and sixth columns show wavelength, wavenumber, and two differences: between the experimental and calculated (by using the experimental energies of the levels involved) wavenumbers and wavelengths. Next two columns, viz. seventh (N_{even}) and eighth (N_{odd}), give information about the even and odd levels involved in the transition: the number of identified spectral lines used to determine the level. In the ninth and tenth columns we give the names of the configurations and energy values for the even and odd levels involved in the transition, respectively. For the even levels the names of the levels are also given. For the odd levels the J -values of the levels are shown in brackets. The last column contains remarks. Lines marked by "c" and "d" in this column are respectively from Ref. [9] and Ref.

[3] As can be seen from Table I, the finally achieved relative accuracy of wavelengths in the main list (1204–2445 Å) is 0.004 Å. The accuracy of the lines above 2445 Å [3] is about 0.017 Å. Lines below 1200 Å [9] have a systematic error of 0.013 Å with an additional random component of 0.010 Å. One may notice in Table I twelve pairs of close lines which, due to the large dispersion of the spectrograph, exhibit resolved hyperfine structures (see next section).

All the 37 levels of the $5d^3$, $5d^26s$ and $5d6s^2$ configurations and all the 68 levels of the $5d^26p$ and $5d6s6p$ configurations have been established. The even levels are determined by 4–39 (by 19 in average) transitions. The odd levels are based on 2–18 (on 11 in average) spectral lines. These numbers show that the reliability of the analysis is quite high. Experimental and calculated energy values of the even parity levels in the $5d^3$, $5d^26s$ and $5d6s^2$ configurations and the odd parity levels in the $5d^26p$, $5d6s6p$ and $6s^26p$ configurations of Ta III are given respectively in Table II and Table III. The first three columns of the tables show the observed and calculated energy values of levels and also the difference between these values. In the fourth column we give the number of identified spectral lines used to determine the level. The fifth column lists the root-mean-squares (rms) deviation of the energy values calculated from wavenumbers by excluding masked, blended and multiply identified lines. The calculated Landé factors, g , of levels are given in the sixth column. In the last columns of the two tables the compositions of eigenvectors are given. In the odd system many main components are below 50%, with the lowest being 19%. Due to the strong level mixing, the LS -notation for odd levels have not been given in Table I. The uncertainty in the adopted energy values of the 102 established levels is 0.05–0.16 cm^{-1} , and does not exceed 0.10 cm^{-1} for 90% of them. Only three levels are determined with a rms deviation of 0.20–0.30 cm^{-1} .

All the semiempirical calculations (fitting) were carried out by using the orthogonal operator technique [16,20,21]. Some parameters of the studied configurations, all the parameters of the unknown configuration $6s^26p$ and also three configuration interaction parameters in the odd system were kept fixed at the predetermined values during the fitting procedure. In Table IV and Table V the parameters obtained (or used fixed) in the calculations for the even and odd systems are presented. The second columns of the tables show the parameter values obtained in the final least-squares fit (LSF). Values in brackets are the uncertainties of the fitted parameter values. In the third columns the *ab initio* values of the parameters calculated using the Hartree–Fock method with relativistic correction (HFR) [19] are presented. The obtained (or predetermined and fixed) scaling factors (LSF/HFR) are shown in the fourth columns of Table IV and Table V.

6. Hyperfine structure

As mentioned before, twelve hyperfine structures can be seen in Table I. Natural tantalum, of which our light source is made, is almost pure ^{181}Ta isotope (99.978%) with a nuclear spin $I = 7/2$ and a nuclear magnetic moment $\mu = 2.3 \text{ nm}$. In the case of neutral tantalum (Ta I) studied with atomic beam LIF techniques, lines exhibit hyperfine

Table I. Continued.

$\frac{gA}{(10^7 \text{ s}^{-1})}$	Int	λ (Å)	ν (cm ⁻¹)	$\Delta(\nu)^a$ (cm ⁻¹)	$\Delta(\lambda)^a$ (Å)	N_{even}^b	N_{odd}^b	Even level	Odd level	Remark			
1	4	2726.852	36661.47	-0.24	0.018	24	14	5d ² 6s (¹ D)	² D _{5/2}	25781.52	5d ² 6p	62443.23(5/2)	d
5	2	2730.976	36606.11	-0.43	0.032	18	15	5d ³	² F _{7/2}	29375.47	5d ² 6p	65982.01(7/2)	d
1	2	2737.199	36522.89	0.07	-0.005	26	9	5d ³	⁴ P _{3/2}	15681.10	5d ² 6p	52203.92(3/2)	d
9	25	2740.110	36484.09	0.02	-0.002	33	9	5d ² 6s (³ F)	² F _{5/2}	15719.85	5d ² 6p	52203.92(3/2)	d
2	15	2742.234	36455.83	0.19	-0.014	19	15	5d6s ²	² D _{3/2}	28408.19	5d ² 6p	64863.83(3/2)	d
2	2	2772.056	36063.66	0.19	-0.015	39	7	5d ³	³ D _{5/2}	12134.38	5d ² 6p	48197.85(5/2)	d
4	5	2773.595	36043.65	0.13	-0.010	29	11	5d ² 6s (³ F)	² F _{7/2}	17906.64	5d ² 6p	53950.16(7/2)	d
11	5	2776.231	36009.42	-0.02	0.001	13	10	5d ² 6s (¹ G)	² G _{9/2}	27329.62	5d ² 6p	63339.06(9/2)	d
1	3	2804.580	35645.46	0.09	-0.007	19	17	5d6s ²	² D _{3/2}	28408.19	5d ² 6p	64053.56(5/2)	d
1	6	2854.786	35018.60	0.48	-0.039	18	15	5d ³	² F _{7/2}	29375.47	5d ² 6p	64393.59(7/2)	d
4	8	2882.826	34678.01	-0.08	0.006	18	17	5d ³	² F _{7/2}	29375.47	5d ² 6p	64053.56(5/2)	d
4	7	2896.041	34519.78	-0.08	0.006	22	9	5d ² 6s (¹ D)	² D _{3/2}	23796.27	5d ² 6p	58316.13(3/2)	d
5	5	2943.482	33963.44	-0.15	0.013	18	10	5d ³	² F _{7/2}	29375.47	5d ² 6p	63339.06(9/2)	d
2	8	2954.921	33831.97	-0.32	0.028	32	7	5d ³	⁴ P _{5/2}	14365.56	5d ² 6p	48197.85(5/2)	d
5	100	2956.835	33810.07	0.08	-0.007	22	11	5d ² 6s (¹ D)	² D _{3/2}	23796.27	5d ² 6p	57606.26(5/2)	d
4	8	3019.336	33110.22	0.06	-0.005	19	13	5d ² 6s (¹ G)	² G _{7/2}	26971.24	5d ² 6p	60081.40(7/2)	d
4	5	3023.202	33067.88	0.12	-0.011	18	14	5d ³	² F _{7/2}	29375.47	5d ² 6p	62443.23(5/2)	d
6	25	3078.097	32478.17	0.17	-0.016	33	7	5d ² 6s (³ F)	² F _{5/2}	15719.85	5d ² 6p	48197.85(5/2)	d
7	10	3088.692	32366.77	-0.05	0.005	18	11	5d ³	² F _{7/2}	29375.47	5d ² 6p	61742.29(7/2)	d
1	3	3132.861	31910.46	-0.01	0.001	10	15	5d ² 6s (³ P)	² P _{1/2}	32953.36	5d ² 6p	64863.83(3/2)	d
3	15	3164.345	31592.97	0.09	-0.009	22	13	5d ² 6s (¹ D)	² D _{3/2}	23796.27	5d ² 6p	55389.15(5/2)	d
5	10	3177.564	31461.55	0.06	-0.006	24	9	5d ³	² F _{5/2}	26854.64	5d ² 6p	58316.13(3/2)	d
4	12	3255.760	30705.94	0.01	-0.001	18	13	5d ³	² F _{7/2}	29375.47	5d ² 6p	60081.40(7/2)	d
4	10	3288.566	30399.63	0.03	-0.004	10	14	5d ² 6s (³ P)	² P _{1/2}	32953.36	5d ² 6p	63352.96(3/2)	d
4	12	3290.764	30379.33	-0.09	0.010	18	14	5d6s ²	² D _{5/2}	32063.81	5d ² 6p	62443.23(5/2)	d
1	6	3524.550	28364.31	0.15	-0.019	14	15	5d ² 6s (³ P)	² P _{3/2}	36499.67	5d ² 6p	64863.83(3/2)	d
2	10	3569.817	28004.64	0.10	-0.013	10	5	5d ² 6s (³ P)	² P _{1/2}	32953.36	5d ² 6p	60957.90(1/2)	d
2	8	3689.597	27095.52	0.00	0.000	24	11	5d ³	² F _{5/2}	26854.64	5d ² 6p	53950.16(7/2)	d
2	2	3843.023	26013.80	0.12	-0.018	18	13	5d ³	² F _{7/2}	29375.47	5d ² 6p	55389.15(5/2)	d
2	10	3856.328	25924.05	0.05	-0.008	14	9	5d ² 6s (³ P)	² P _{3/2}	36499.67	5d ² 6p	62423.67(1/2)	d
2	10	3943.777	25349.23	-0.05	0.008	24	9	5d ³	² F _{5/2}	26854.64	5d ² 6p	52203.92(3/2)	d

^a $\Delta(x)$ = Difference between the observed and calculated (derived from the level energies) values of x .

^b $N_{\text{odd}}, N_{\text{even}}$ = The number of observed transitions from (to) the level involved, respectively.

^c Lines are from Ref. [9]

^d Lines are from Ref. [3]

M = The Ta III line is masked by some other line.

Str = The intensity of the line is too strong compared to expected (2–3 times).

Bl = The line is blended by a close line.

Hfs = Hyperfine splitting of the 5d²6s (³P)⁴P_{1/2} energy level at 17030.94 cm⁻¹.

F = F -values correspond to the two hfs sublevels (43279.83 cm⁻¹ and 43281.99 cm⁻¹) of the 5d²6s (¹S)²S_{1/2} energy level.

structures (hfs) which have been interpreted theoretically [24]. The magnetic hfs constants in the low even group (5d + 6s)⁵ are expressed in terms of adjustable mono-electronic parameters a_{5d}^{ek} and a_{6s}^{10} which dominates the former ones by a factor of twenty. As concerns ions of the 5d-elements, Fourier Transform spectrometry (FTS) resumed high resolution studies, which were initiated long ago by Fabry–Perot interferometry, but results on Ta III did not appear so far. Semi-empirical considerations help to evaluate the sizes of the structures in the present work. The mono-electronic parameters scale as $\langle r^{-3} \rangle$ and are expected to increase with ionic charge. This trend is confirmed in the nearby element $_{71}\text{Lu}$. FTS analysis of Lu I [25] and subsequent interpretation of (5d + 6s)³ and (5d + 6s)²6p led to $a_{6s}^{10} = 0.275 \pm 0.002 \text{ cm}^{-1}$ [26]. The observation of the Lu III 6s²S–6p²P doublet on the 10.7 m spectrograph at the National Bureau of Standards (NBS) (similar to the one in Meudon, with a 1200 lines/mm ruled grating) led Kaufman and Sugar to $0.436 \pm 0.002 \text{ cm}^{-1}$ for the same parameter [27]. In Lu II, Gollnow derived intermediate values 0.362 cm^{-1} from 6s6p and 0.320 cm^{-1} from 5d6s [28]. In Ta I, a value $a_{6s}^{10} = 0.306 \pm 0.005 \text{ cm}^{-1}$ is derived in [24] and for Ta II Murakawa obtained $0.405 \pm 0.005 \text{ cm}^{-1}$ from the A -con-

stant of the ground level 5d³6s⁵F₁ [29], in agreement with *ab initio* studies [30], provided that the results are scaled from nuclear spin $I = 3/2$ to $I = 7/2$. Recent refinement of the energy level structure of Ta II and careful analysis of hfs patterns of Ta II by means of FTS resulted in a list of well defined hfs constants for 105 levels [31]. These

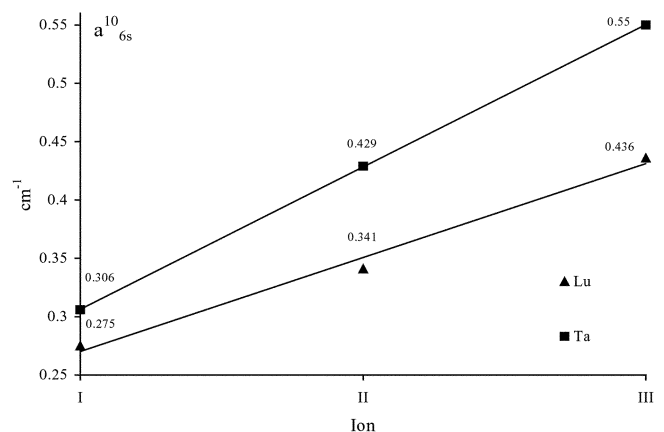


Fig. 1. Estimation of an a_{6s}^{10} value for Ta III. Data on Lu I – Lu III, Ta I and Ta II are used.

Table II. Experimental and calculated energy levels (cm^{-1}) in the $5d^3$, $5d^26s$ and $5d6s^2$ configurations of Ta III.

E_{obs}	E_{calc}	Δ^a	N^b	rms	g^c	Composition ^d							
$J = 0.5$													
43281.18	43381.08	-99.90	4	0.13	1.938	92%	$2 \left(\frac{1}{2}S\right) ^2S$	+	5%	$2 \left(\frac{3}{2}P\right) ^2P$	+	2%	$2 \left(\frac{3}{2}P\right) ^4P$
32953.36	33013.01	-59.65	10	0.10	0.757	71%	$2 \left(\frac{3}{2}P\right) ^2P$	+	23%	$1 \left(\frac{3}{2}P\right) ^2P$	+	5%	$2 \left(\frac{1}{2}S\right) ^2S$
17030.94	17122.01	-91.07	14	0.30	2.639	97%	$2 \left(\frac{3}{2}P\right) ^4P$	+	3%	$2 \left(\frac{1}{2}S\right) ^2S$	+	1%	$1 \left(\frac{3}{2}P\right) ^2P$
12805.56	12786.25	19.31	10	0.06	2.215	77%	$1 \left(\frac{4}{3}P\right) ^4P$	+	15%	$1 \left(\frac{3}{2}P\right) ^2P$	+	8%	$2 \left(\frac{3}{2}P\right) ^2P$
7882.85	7849.07	33.78	13	0.06	1.126	60%	$1 \left(\frac{2}{3}P\right) ^2P$	+	23%	$1 \left(\frac{4}{3}P\right) ^4P$	+	17%	$2 \left(\frac{3}{2}P\right) ^2P$
$J = 1.5$													
40470.77	40426.30	44.47	6	0.05	0.808	51%	$1 \left(\frac{2}{1}D\right) ^2D$	+	28%	$3 \left(\frac{2}{1}D\right) ^2D$	+	17%	$1 \left(\frac{2}{3}D\right) ^2D$
36499.67	36477.56	22.11	14	0.14	1.295	69%	$2 \left(\frac{3}{2}P\right) ^2P$	+	22%	$1 \left(\frac{3}{2}P\right) ^2P$	+	4%	$2 \left(\frac{1}{2}D\right) ^2D$
28408.19	28428.15	-19.96	19	0.08	0.810	53%	$3 \left(\frac{2}{1}D\right) ^2D$	+	17%	$1 \left(\frac{2}{1}D\right) ^2D$	+	16%	$2 \left(\frac{1}{2}D\right) ^2D$
23796.27	23735.69	60.58	22	0.07	0.839	46%	$2 \left(\frac{1}{2}D\right) ^2D$	+	30%	$1 \left(\frac{3}{2}D\right) ^2D$	+	8%	$3 \left(\frac{2}{1}D\right) ^2D$
18777.41	18811.59	-34.18	23	0.05	1.687	93%	$2 \left(\frac{3}{2}P\right) ^4P$	+	2%	$1 \left(\frac{3}{2}D\right) ^2D$	+	2%	$1 \left(\frac{3}{2}P\right) ^2P$
15681.10	15778.66	-97.56	26	0.06	1.385	35%	$1 \left(\frac{4}{3}P\right) ^4P$	+	30%	$1 \left(\frac{3}{2}P\right) ^2P$	+	13%	$2 \left(\frac{3}{2}P\right) ^2P$
12626.87	12689.94	-63.07	23	0.06	1.171	42%	$1 \left(\frac{4}{3}P\right) ^4P$	+	19%	$1 \left(\frac{3}{2}D\right) ^2D$	+	15%	$2 \left(\frac{1}{2}D\right) ^2D$
7186.97	7164.23	22.74	28	0.06	1.073	34%	$1 \left(\frac{3}{2}P\right) ^2P$	+	27%	$2 \left(\frac{3}{2}F\right) ^4F$	+	19%	$1 \left(\frac{4}{3}P\right) ^4P$
5542.39	5539.41	2.98	27	0.08	0.597	66%	$2 \left(\frac{3}{2}F\right) ^4F$	+	9%	$2 \left(\frac{1}{2}D\right) ^2D$	+	8%	$1 \left(\frac{2}{3}P\right) ^2P$
0.00	21.68	-21.68	16	0.07	0.469	85%	$1 \left(\frac{4}{3}F\right) ^4F$	+	7%	$1 \left(\frac{3}{2}D\right) ^2D$	+	4%	$1 \left(\frac{2}{1}D\right) ^2D$
$J = 2.5$													
42619.53	42655.48	-35.95	4	0.08	1.197	49%	$3 \left(\frac{2}{1}D\right) ^2D$	+	42%	$1 \left(\frac{2}{1}D\right) ^2D$	+	4%	$1 \left(\frac{2}{3}D\right) ^2D$
32063.81	32002.27	61.54	18	0.07	1.131	31%	$3 \left(\frac{2}{1}D\right) ^2D$	+	29%	$1 \left(\frac{2}{1}D\right) ^2D$	+	17%	$1 \left(\frac{2}{3}F\right) ^2F$
26854.64	26890.01	-35.37	24	0.06	0.973	48%	$1 \left(\frac{2}{3}F\right) ^2F$	+	19%	$2 \left(\frac{3}{2}F\right) ^2F$	+	12%	$1 \left(\frac{2}{1}D\right) ^2D$
25781.52	25684.16	97.36	24	0.06	1.219	40%	$2 \left(\frac{1}{2}D\right) ^2D$	+	27%	$1 \left(\frac{3}{2}D\right) ^2D$	+	14%	$2 \left(\frac{3}{2}P\right) ^4P$
20102.95	20071.75	31.20	25	0.08	1.513	78%	$2 \left(\frac{3}{2}P\right) ^4P$	+	16%	$1 \left(\frac{3}{2}D\right) ^2D$	+	3%	$1 \left(\frac{2}{1}D\right) ^2D$
15719.85	15688.00	31.85	33	0.05	0.995	51%	$2 \left(\frac{3}{2}F\right) ^2F$	+	16%	$1 \left(\frac{2}{3}F\right) ^2F$	+	14%	$1 \left(\frac{2}{3}D\right) ^2D$
14365.56	14315.01	50.55	32	0.09	1.452	75%	$1 \left(\frac{4}{3}P\right) ^4P$	+	11%	$2 \left(\frac{3}{2}F\right) ^2F$	+	5%	$2 \left(\frac{1}{2}D\right) ^2D$
12134.38	12222.26	-87.88	39	0.07	1.222	21%	$2 \left(\frac{1}{2}D\right) ^2D$	+	19%	$1 \left(\frac{3}{2}D\right) ^2D$	+	18%	$1 \left(\frac{4}{3}P\right) ^4P$
7305.09	7331.65	-26.56	28	0.07	1.037	81%	$2 \left(\frac{3}{2}F\right) ^4F$	+	8%	$2 \left(\frac{1}{2}D\right) ^2D$	+	7%	$2 \left(\frac{3}{2}F\right) ^2F$
2512.43	2524.45	-12.02	17	0.07	1.036	96%	$1 \left(\frac{4}{3}F\right) ^4F$	+	3%	$1 \left(\frac{3}{2}D\right) ^2D$	+	1%	$1 \left(\frac{2}{1}D\right) ^2D$
$J = 3.5$													
29375.47	29496.16	-120.69	18	0.09	1.111	43%	$2 \left(\frac{3}{2}F\right) ^2F$	+	43%	$1 \left(\frac{2}{3}F\right) ^2F$	+	13%	$2 \left(\frac{1}{2}G\right) ^2G$
26971.24	26901.47	69.77	19	0.05	0.930	76%	$2 \left(\frac{1}{2}G\right) ^2G$	+	15%	$1 \left(\frac{2}{3}F\right) ^2F$	+	8%	$1 \left(\frac{2}{3}G\right) ^2G$
17906.64	17851.33	55.31	29	0.06	1.135	52%	$2 \left(\frac{3}{2}F\right) ^2F$	+	40%	$1 \left(\frac{3}{2}F\right) ^2F$	+	4%	$2 \left(\frac{1}{2}G\right) ^2G$
11296.10	11304.21	-8.11	22	0.06	0.953	76%	$1 \left(\frac{2}{3}G\right) ^2G$	+	12%	$2 \left(\frac{3}{2}F\right) ^4F$	+	6%	$1 \left(\frac{4}{3}F\right) ^4F$
10425.17	10418.78	6.39	27	0.07	1.197	84%	$2 \left(\frac{3}{2}F\right) ^4F$	+	9%	$1 \left(\frac{2}{3}G\right) ^2G$	+	3%	$2 \left(\frac{3}{2}F\right) ^2F$
4854.18	4854.23	-0.05	18	0.07	1.215	93%	$1 \left(\frac{4}{3}F\right) ^4F$	+	6%	$1 \left(\frac{3}{2}G\right) ^2G$	+	1%	$1 \left(\frac{2}{3}F\right) ^2F$
$J = 4.5$													
27329.62	27315.63	13.99	13	0.08	1.115	85%	$2 \left(\frac{1}{2}G\right) ^2G$	+	11%	$1 \left(\frac{2}{3}G\right) ^2G$	+	2%	$2 \left(\frac{3}{2}F\right) ^4F$
17800.85	17826.57	-25.72	15	0.06	1.015	54%	$1 \left(\frac{2}{3}H\right) ^2H$	+	33%	$1 \left(\frac{2}{3}G\right) ^2G$	+	7%	$2 \left(\frac{1}{2}G\right) ^2G$
13766.13	13780.35	-14.22	14	0.06	1.293	88%	$2 \left(\frac{3}{2}F\right) ^4F$	+	8%	$1 \left(\frac{2}{3}H\right) ^2H$	+	2%	$1 \left(\frac{2}{3}G\right) ^2G$
12350.26	12310.26	40.00	17	0.07	1.100	35%	$1 \left(\frac{2}{3}H\right) ^2H$	+	34%	$1 \left(\frac{2}{3}G\right) ^2G$	+	19%	$1 \left(\frac{4}{3}F\right) ^4F$
6776.24	6759.70	16.54	15	0.07	1.277	77%	$1 \left(\frac{4}{3}F\right) ^4F$	+	20%	$1 \left(\frac{2}{3}G\right) ^2G$	+	3%	$1 \left(\frac{2}{3}H\right) ^2H$
$J = 5.5$													
17553.75	17557.70	-3.95	5	0.05	1.091	100%	$1 \left(\frac{2}{3}H\right) ^2H$						

^a $\Delta = (E_{\text{obs}} - E_{\text{calc}})$.

^b N = The number of spectral lines used to determine the energy level value.

^c g = The calculated Landé factor.

^d The number preceding the term name has the following meaning: 1 stands for $5d^3$, 2 stands for $5d^26s$, and 3 stands for $5d6s^2$.

constants determine a new value, $a_{6s}^{10} = 0.429 \pm 0.01 \text{ cm}^{-1}$, for Ta II. All these data were used to estimate a a_{6s}^{10} value in Ta III (see Fig. 1). For Lu II we used a value of 0.341 cm^{-1} which is the average of those two published [28]. The regular trends that can be seen in Fig. 1 lead to an expected value $a_{6s}^{10} = 0.55 \pm 0.01 \text{ cm}^{-1}$ in Ta III, and for the level $5d^26s^2S_{1/2}$ the hfs splitting is $4 \times a_{6s}^{10} = 2.20 \text{ cm}^{-1}$. This is consistent with the present observations. The search for the level $5d^26s^2S_{1/2}$ leads to the two values $43279.83 \pm 0.05 \text{ cm}^{-1}$ and $43281.99 \pm 0.08 \text{ cm}^{-1}$ corresponding to hfs transitions towards $F = 3$ and $F = 4$ of $^2S_{1/2}$ sublevels respectively. The derived value of the $^2S_{1/2}$

level and the value of the splitting are $43281.18 \pm 0.13 \text{ cm}^{-1}$ and $2.18 \pm 0.11 \text{ cm}^{-1}$. Due to different C.I. effects and coupling conditions, comparisons of Ta III with Lu I are not straightforward. It is noticed that two other levels ($5d^26s^4P_{1/2}$ and $5d6s6p^4P_{1/2}$) have prominent A constants in Lu I. In Ta III the former of both levels (17030.94 cm^{-1}) has partially resolved hfs transitions, doublet-like with average separation of $1.14 \pm 0.15 \text{ cm}^{-1}$. Other transitions with larger J -values and smaller A constants are expected to have more complex hfs patterns which contribute to the asymmetry of several lines and merge into wavenumber uncertainties.

Table III. Continued.

E_{obs}	E_{calc}	Δ^a	N^b	rms	g^c	Composition ^d							
$J = 4.5$													
80061.85	80151.54	-89.69	7	0.08	1.334	98%	2 ($\frac{3}{2}\text{D}$) ^4F	+	1%	1 ($\frac{3}{2}\text{F}$) ^4F	+	1%	1 ($\frac{1}{2}\text{G}$) ^2G
75519.76	75563.05	-43.29	7	0.07	1.033	56%	1 ($\frac{1}{2}\text{G}$) ^2G	+	41%	1 ($\frac{1}{2}\text{G}$) ^2H	+	2%	1 ($\frac{3}{2}\text{F}$) ^4F
72393.26	72368.12	25.14	11	0.09	1.092	65%	1 ($\frac{3}{2}\text{F}$) ^2G	+	17%	1 ($\frac{1}{2}\text{G}$) ^2H	+	12%	1 ($\frac{1}{2}\text{G}$) ^2G
68136.41	68089.50	46.91	10	0.09	1.133	41%	1 ($\frac{3}{2}\text{F}$) ^4F	+	35%	1 ($\frac{1}{2}\text{G}$) ^2H	+	16%	1 ($\frac{1}{2}\text{G}$) ^2G
63339.06	63346.79	-7.73	10	0.05	1.201	34%	1 ($\frac{3}{2}\text{F}$) ^4F	+	32%	1 ($\frac{3}{2}\text{F}$) ^4G	+	19%	1 ($\frac{3}{2}\text{F}$) ^2G
58907.94	58846.52	61.42	8	0.06	1.179	68%	1 ($\frac{3}{2}\text{F}$) ^4G	+	15%	1 ($\frac{3}{2}\text{F}$) ^4F	+	9%	1 ($\frac{3}{2}\text{F}$) ^2G
$J = 5.5$													
77747.11	77694.68	52.43	4	0.05	1.098	96%	1 ($\frac{1}{2}\text{G}$) ^2H	+	4%	1 ($\frac{3}{2}\text{F}$) ^4G			
65531.18	65639.20	-108.02	3	0.05	1.267	96%	1 ($\frac{3}{2}\text{F}$) ^4G	+	4%	1 ($\frac{1}{2}\text{G}$) ^2H			

^a $\Delta = (E_{\text{obs}} - E_{\text{calc}})$.

^b N = The number of spectral lines used to determine the energy level value.

^c g = The calculated Landé factor.

^d The number preceding the term name has the following meaning: 1 stands for $5d^26p$, 2 stands for $5d6s6p$, and 3 stands for $6s^26p$.

Table IV. Least-squares fitted (LSF) and calculated parameter values (cm^{-1}) in the $5d^3$, $5d^26s$ and $5d6s^2$ configurations of Ta III.

Parameter	LSF	HFR	LSF/HFR
$5d^3$			
E_{av}	15729.9 (32.4)	19061.4	
O_2	4508.7 (36.9)	5788.7	0.7789
O'_2	3197.7 (27.6)	4005.1	0.7984
E_a	94.9 (28.1)		
E_b	39.1 (40.0)		
ζ_d	1909.4 (18.7)	2141.2	0.8917
A_c	21.6		
A_3	2.4		
A_4	4.2		
A_5	4.3		
A_6	11.7		
A_1	-1.8		
A_2	2.0		
A_0	-1.6		
$5d^26s$			
E_{av}	19548.8 (32.0)	24121.0	0.7548 ^a
O_2	4766.1 (25.8)	6058.0	0.7868
O'_2	3428.9 (35.2)	4171.9	0.8219
E_a	106.6 (41.6)		
E_b	-10.0		
ζ_d	2105.6 (23.4)	2327.2	0.9048
A_c	20.9		
A_3	2.4		
A_4	4.2		
A_5	4.2		
A_6	11.3		
A_1	-1.7		
A_2	1.9		
A_0	-1.5		
C_{ds}	2796.0 (26.5)	3714.0	0.7528
T_{dds}	17.5 (33.7)		
A_{ms0}	49.8 (20.3)		
$5d6s^2$			
E_{av}	33115.3 (270.3)	42313.2	0.7477 ^a
ζ_d	2310.8 (79.4)	2519.3	0.9172
$R^2(\text{dd}, \text{ds})12^b$	-20343.1 (134.9)	-26263.6	0.7746
$R^2(\text{dd}, \text{ss})12$	17141.8 (212.0)	23949.6	0.7157
$R^2(\text{dd}, \text{ds})23$	-19846.7 (878.7)	-26271.8	0.7554
Mean Deviation ^c = 70 cm^{-1}			

^a The energy differences with respect to the ground configuration were used:

$(E_{\text{av}}(\text{conf}) - E_{\text{av}}(5d^3))_{\text{LSF}} / (E_{\text{av}}(\text{conf}) - E_{\text{av}}(5d^3))_{\text{HFR}}$, where "conf" is either $5d^26s$ or $5d6s^2$.

^b "xy" behind the R -integral means interaction between configuration x and y . 1 stands for $5d^3$, 2 stands for $5d^26s$ and 3 stands for $5d6s^2$.

^c Mean Deviation = $[(\sum(E_{\text{obs}} - E_{\text{calc}})^2) / (n - m)]^{1/2}$, where n is the number of known levels, m is the number of free parameters.

Table V. *Least-squares fitted (LSF) and calculated parameter values (cm^{-1}) in the $5d^26p$, $5d6s6p$ and $6s^26p$ configurations of Ta III.*

Parameter	LSF	HFR	LSF/HFR
5d²6p			
E_{av}	68808.2 (52.3)	71171.4	1.0186 ^a
O_2	4719.3 (60.0)	6149.5	0.7674
O'_2	3491.0 (47.3)	4227.9	0.8257
E_a	10.7 (78.9)		
E_b	-91.7 (61.0)		
ζ_d	2245.4 (26.5)	2386.4	0.9409
A_c	21.6		
A_3	2.4		
A_4	4.2		
A_5	4.3		
A_6	11.7		
A_1	-1.8		
A_2	2.0		
A_0	-1.6		
$C_1(\text{dp})$	1899.7 (52.9)	2301.3	0.8255
$C_2(\text{dp})$	2100.0 (62.8)	2907.1	0.7224
$C_3(\text{dp})$	1286.6 (48.3)	1628.8	0.7899
$S_1(\text{dp})$	239.9 (57.5)		
$S_2(\text{dp})$	-112.7 (42.8)		
T_{16}	-25.0		
T_{25}	5.0		
T_{26}	-35.0		
T_{27}	5.0		
T_{28}	55.0		
T_{29}	-35.0		
T_{30}	10.0		
ζ_p	5390.0 (59.0)	4467.4	1.2065
SS_{02}	0.0		
SS_{20}	0.0		
$S_d \cdot L_p$	-90.0		
$S_p \cdot L_d$	-10.0		
$Z_{pp'}^2$	-50.0		
$Z_{dd'}^2$	60.0		
$Z_{pp'}^1$	100.0		
$Z_{dd'}^1$	0.0		
$Z_{pp'}^3$	40.0		
$Z_{dd'}^3$	-30.0		
5d6s6p			
E_{av}	81729.0 (116.3)	85349.8	0.9956 ^a
ζ_d	2536.7 (58.1)	2573.1	0.9859
Cd_s	2904.2 (144.4)	3672.4	0.7908
A_{mso}	52.0		
A_{ss}	0.0		
$C_1(\text{dp})$	2430.1 (83.0)	2483.7	0.9784
$C_2(\text{dp})$	2213.3 (94.0)	2952.9	0.7495
$C_3(\text{dp})$	1623.2 (82.4)	1626.6	0.9979
$S_1(\text{dp})$	-75.6 (66.9)		
$S_2(\text{dp})$	-150.7 (140.6)		
ζ_p	5554.0 (213.6)	5210.3	1.0660
$S_d \cdot L_p$	-90.0		
$S_p \cdot L_d$	-10.0		
$Z_{pp'}^2$	-50.0		
$Z_{dd'}^2$	60.0		
$Z_{pp'}^1$	100.0		
$Z_{dd'}^1$	0.0		
$Z_{pp'}^3$	40.0		
$Z_{dd'}^3$	-30.0		
C_{sp}	6871.7 (118.6)	11446.6	0.6003
$A_{\text{mso}}(\text{sp})$	-615.5 (265.7)		
6s²6p			
E_{av}	105500.0	113571.7	0.9498 ^a
ζ_p	7165.0	6021.2	1.1900
$R^2(\text{dd}, \text{ds})12^b$	-21787.2 (792.2)	-26215.3	0.8311
$R^2(\text{dp}, \text{sp})12$	-14751.3 (435.1)	-21442.2	0.6880
$R^1(\text{dp}, \text{ps})12$	-14024.5 (341.5)	-20439.8	0.6861
$R^2(\text{dd}, \text{ss})13$	16744.0	23728.5	0.7056
$R^2(\text{dp}, \text{sp})23$	-15495.0	-21957.7	0.7057

Table V. *Continued.*

Parameter	LSF	HFR	LSF/HFR
$R^1(\text{dp, ps})_{23}$	-14664.0	-20780.0	0.7057
Mean Deviation ^c = 126 cm ⁻¹			

^a The energy differences with respect to the ground configuration were used: $(E_{\text{av}}(\text{conf}) - E_{\text{av}}(5d^3))_{\text{LSF}} / (E_{\text{av}}(\text{conf}) - E_{\text{av}}(5d^3))_{\text{HFR}}$, where “conf” is either $5d^26p$, $5d6s6p$ or $6s^26p$.

^b “xy” behind the R -integral means interaction between configuration x and y . 1 stands for $5d^26p$, 2 stands for $5d6s6p$ and 3 stands for $6s^26p$.

^c Mean Deviation = $[(\sum(E_{\text{obs}} - E_{\text{calc}})^2)/(n - m)]^{1/2}$, where n is the number of known levels, m is the number of free parameters.

Acknowledgements

It is a pleasure for VIA to acknowledge the hospitality received from the Paris-Meudon Observatory, France, during his visit. Dr. P. H. M. Uylings and Dr. A. J. J. Raassen are acknowledged for permission to use their codes for orthogonal parameter calculations. WLTB would like to acknowledge M. Benharrous for technical assistance and F. Launay for her help in operating the 10m spectrograph. This work has been supported by the “Programme National de Physique Stellaire” of the Centre National de Recherche Scientifique (CNRS).

References

- Leckrone, D. S., Wahlgren, G. M. and Johansson, S. G., *Astrophys. J.* **377**, L37 (1991).
- Leckrone, D. S., Proffitt, C. R., Wahlgren, G. M., Johansson, S. G. and Brage, T., *Astronomical J.* **117**, 1454 (1999).
- Kiess, C. C., *J. Res. NBS A*, **66A**, 111 (1962).
- Meijer, F. G. and Metsch, B. C., *Physica* **94C**, 259 (1978).
- Meijer, F. G. and Klinkenberg, P. F. A., *Physica* **69**, 111 (1973).
- Kaufman, V. and Sugar, J., *J. Opt. Soc. Am.* **65**, 302 (1975).
- Kildiyarova, R. R., Churilov, S. S. and Joshi, Y. N., *Physica Scripta* **53**, 454, (1996).
- Tchang-Brillet, W.-Ü L. and Azarov, V. I., *Physica Scripta* **T100**, 104 (2002).
- Meijer, F. G., Unpublished Zeeman laboratory measurements.
- Azarov, V. I., *J. Opt. Soc. Am. B* **18**, 106 (2001).
- Iglesias, L., Kaufman, V., Garcia-Riquelme, O. and Rico, F. R., *Physica Scripta* **31**, 173 (1985).
- Kildiyarova, R. R., *Physica Scripta* **53**, 668 (1998).
- Raassen, A. J. J. *et al.*, *Physica Scripta* **54**, 56 (1996).
- Kildiyarova, R. R., Churilov, S. S. and Joshi, Y. N., *Physica Scripta* **58**, 32 (1998).
- Azarov, V. I., Churilov, S. S. and Joshi, Y. N., *Physica Scripta* **60**, 506 (1999).
- Uylings, P. H. M., Raassen, A. J. J. and Wyart, J.-F., *J. Phys. B: At. Mol. Opt. Phys.* **26**, 4683 (1993).
- Wyart, J.-F., Raassen, A. J. J., Uylings, P. H. M. and Joshi, Y. N., *Physica Scripta* **T47**, 59 (1993).
- Wyart, J.-F. and Blaise, J., *Physica Scripta* **42**, 209 (1990).
- Cowan, R. D., “The Theory of Atomic Structure and Spectra.” (University of California Press, Berkeley, California, 1981), and Cowan Computer Code as modified by Yu. V. Ralchenko and A. E. Kramida of the Institute of Spectroscopy, Troitsk, Russia.
- Hansen, J. E., Uylings, P. H. M. and Raassen, A. J. J., *Physica Scripta* **37**, 664 (1988).
- Hansen, J. E., Raassen, A. J. J., Uylings, P. H. M. and Lister, G. M. S., *Nucl. Instr. Meth. B* **31**, 134 (1988).
- Azarov, V. I., *Physica Scripta* **44**, 528 (1991).
- Azarov, V. I., *Physica Scripta* **48**, 656 (1993).
- Dembczynski, J., Arcimowicz, B., Guthorlein, G. H. and Windholz, L., *Z. Phys. D* **39**, 143 (1997).
- Vergès, J. and Wyart, J.-F., *Physica Scripta* **17**, 495 (1978).
- Wyart, J.-F., *Physica Scripta* **18**, 87 (1978).
- Kaufman, V. and Sugar, J., *J. Opt. Soc. Am.* **61**, 1693 (1971).
- Gollnow, H., *Z. Phys.* **103**, 443 (1936).
- Murakawa, K., *Phys. Rev.* **110**, 393 (1958).
- Norquist, P. L. and Beck, D. R., *J. Phys. B: At. Mol. Opt. Phys.* **34**, 2107 (2001).
- Eriksson, M., Litzén, U., Wahlgren, G. M. and Leckrone, D. S., *Physica Scripta* **65**, 480 (2002).